NENE 2015 September 14-17 PORTOROŽ SLOVENIA
24th International Conference Nuclear Energy for New Europe

Spectral Element Direct Numerical Simulation of Heat Transfer in Turbulent Channel Sodium Flow

Jure Oder, Jernej Urankar, Iztok Tiselj
Jožef Stefan Institute
Jamova cesta 39
SI-1000, Ljubljana, Slovenia
jure.oder@ijs.si, jernej.urankar@student.fmf.uni-lj.si, iztok.tiselj@ijs.si

ABSTRACT

Phénix was a prototype fast breeder reactor that was in operation between the year 1973 and 2009. It was a pool-type reactor cooled with liquid sodium. The net power generating capacity was around 230 MW and the breeding ratio of about 1.12. Because of high thermal conductivity of sodium and liquid metals in general, thermal fluctuations in the liquid can penetrate into adjacent structures with low attenuation. Due to the turbulent nature of the flow, the thermal fluctuations at some point have a typical frequency of 1 Hz. Together with high thermal conductivity these thermal loads cause quick ageing of materials. In this paper we present the direct numerical simulations of fully developed turbulent flow in a channel between two plates with finite dimensions. The outer walls of solid plates are heated with constant flux. In the two other directions, periodic boundary conditions are used. To thermally couple the walls with the fluid, conjugate heat transfer model is used. To compare the results to the past results, gravity is neglected and the temperature is a passive scalar. Simulations are performed with the Nek5000 code. The most notable feature of this code is the use of spectral elements to solve for velocity, temperature and any other passive scalar. Results are compared with simulations based on spectral schemes performed within the THINS EU project between 2010 and 2014. This work is part of work that is performed within the SESAME project of Horizon2020 research programme and is a continuation of research at our department.

1 INTRODUCTION

In the last decades Direct Numerical Simulation (DNS) became an important research tool of the turbulent heat transfer [1]. Particular attention was paid to the DNS of the fully developed turbulent channel flow, as it reveals the basic mechanisms of the convective heat transfer between the fluid and the solid wall. In the recent decade, this topic is becoming more important also in the field of nuclear engineering, where it is used to study thermal fatigue related problems [2], [3]. The first DNSs of heat transfer in the channel flow were made by Kim and Moin [4] in 1989 and Kasagi et al. [5] in 1992. They were followed by a significant number of simulations performed at various Reynolds and Prandtl numbers [6].

To reveal the details of the heat transfer near the wall with a given thickness and material properties (density ρ_w, specific heat c_{pw}, thermal conductivity λ_w) a coupled problem of turbulent heat transfer and unsteady heat conduction in the solid wall has to be solved. Experimental and numerical studies of such conjugate heat transfer can be found in [7] and [8], respectively. They showed analytically and experimentally, that the temperature fluctuations on the fluid-solid interface differ for different fluid-solid systems.

In the present work DNS coupled with unsteady heat conduction in the wall was implemented similarly to the coupling implemented in [8] and [9]. Simulations were performed at constant Prandtl number 0.01, which roughly corresponds to the Prandtl number of the liquid sodium, and at friction Reynolds number $\mathrm{Re}_\tau = 180$. Thickness of the heated wall was assumed to be the same as the half-thickness of the channel, while the material properties: density, specific heat capacity and heat conductivity of the solid were assumed to be the same as in the fluid.

Simulations presented in this work were performed with the numerical code Nek5000 [10], which is based on spectral element method. The spectral element code is validated with results of our previous simulations [9] obtained with the spectral method code. Implementation of the spectral element code is part of our efforts within the Horizon2020 project SESAME, where we intend to use spectral elements to analyse the conjugate heat transfer in the backward facing step geometry, where spectral methods limited to very simple geometries cannot be applied.

2 MATHEMATICAL MODEL

The flow in the channel is assumed to be fully developed. Both walls are assumed to have the same thickness, identical material properties, and the same constant volumetric heat source. The computational domain is shown in Fig. 1.

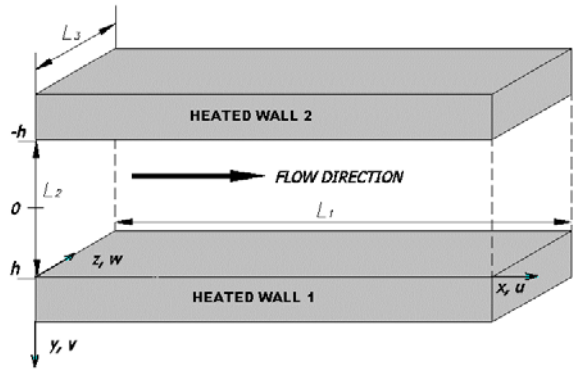

Figure 1: Computational domain. x, y and z mark the three directions of coordinate axes, while u, v and w mark the components of velocity. Flow is directed toward the positive x axis.

The governing equations of the fluid, normalized with channel half width h, friction velocity u_τ, kinematic viscosity ν, and friction temperature $T_\tau = q_w/(u_\tau \rho_f c_{pf})$ can be found in the paper of Monod [11]:

$$\boldsymbol{\nabla} \cdot \boldsymbol{u}^+ = 0, \tag{1}$$

$$\frac{\partial \boldsymbol{u}^+}{\partial t} = -\boldsymbol{\nabla} \cdot (\boldsymbol{u}^+ \boldsymbol{u}^+) + \frac{1}{\mathrm{Re}_\tau} \nabla^2 \boldsymbol{u}^+ - \boldsymbol{\nabla} p + \mathbf{1}_x, \tag{2}$$

$$\frac{\partial \theta^+}{\partial t} = -\boldsymbol{\nabla} \cdot (\boldsymbol{u}^+ \theta^+) + \frac{1}{\mathrm{Re}_\tau \cdot \mathrm{Pr}} \nabla^2 \theta^+ + \frac{u_x^+}{u_B^+}. \tag{3}$$

As can be seen from Eqs. (1)-(3) temperature is assumed to be a passive scalar (there are no terms that would cause natural convection). Dimensionless equation of heat conduction in the wall with internal heating is:

$$\frac{\partial \theta^+}{\partial t} = \frac{1}{G \cdot \mathrm{Re}_\tau \cdot \mathrm{Pr}} \nabla^2 \theta^+ - \frac{K}{d^+ \sqrt{G}}\,, \tag{4}$$

where $-K/(d^+\sqrt{G})$ represents dimensionless internal heat source, in particular:

$$K = \sqrt{\frac{\rho_f c_{pf} \lambda_f}{\rho_w c_{pw} \lambda_w}} \qquad \text{is the thermal activity ratio,} \tag{5}$$

$$G = \frac{\alpha_f}{\alpha_w} \qquad \text{is the thermal diffusivity ratio,} \tag{6}$$

and d^+ is the dimensionless thickness of the wall. At the solid-fluid interface the boundary conditions for temperature and heat flux are:

$$\theta_f^+ = \theta_w^+, \qquad K\sqrt{G}\frac{\partial \theta_f^+}{\partial y^+} = \frac{\partial \theta_w^+}{\partial y^+}, \qquad K\sqrt{G} = \frac{\lambda_f}{\lambda_w}. \tag{7}$$

The outer wall boundaries are assumed to be adiabatic. For liquid sodium - stainless stell wall these values are around $K \approx 1$ and $G \approx 10$. In the present paper the code was validated for the case where $K = 1$, $G = 1$, $d^+ = \mathrm{Re}_\tau = 180$, and $\mathrm{Pr} = 0.01$.

The whole fluid-solid system is adiabatic in the long time average, however, since it does not have a point with a fixed temperature, the mean system temperature slightly fluctuates in time due to the small variations in the efficiency of the turbulent heat transfer. The system temperature presented in the Figures below is shifted with a value that moves the average temperature at the fluid-solid contact planes to zero.

3 NUMERICAL PROCEDURES

The fluid equations are solved with spectral element scheme implemented in the computer code Nek5000 [10,12] and compared with our previous result [9] that were obtained with spectral scheme within the THINS EU project between 2010 and 2014.

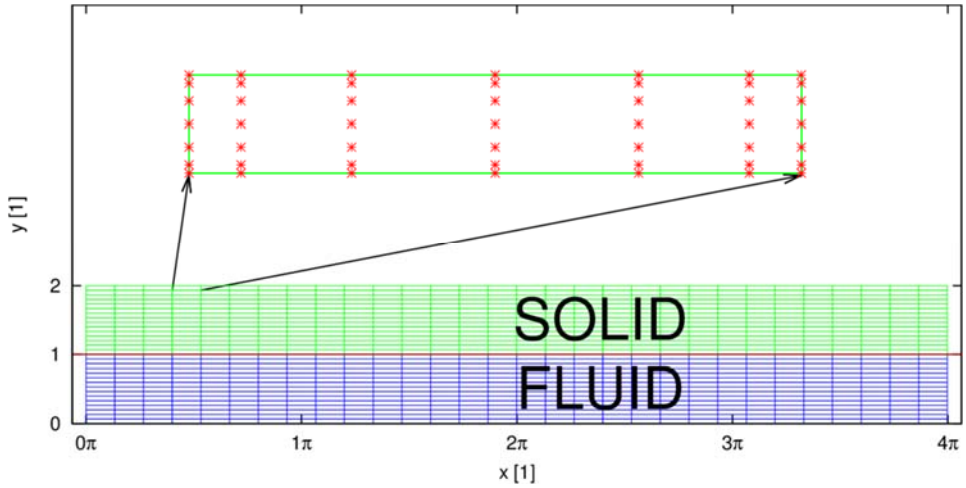

Figure 2: Bottom: half of the computational domain (2D projection) divided into spectral elements. Top: one spectral element of the 6th order (2D projection) with GLL points.

Spectral element method is a type of spatial discretization technique, using method of weighted residuals. It is a class of finite element method which uses polynomials as basic

functions. These functions are often Lagrange, Legendre or Chebyschev polynomials. Application Nek5000 divides space into two domains – fluid and solid. Each domain is subdivided into elements which are box-shaped (Tab. 1). Application sets Gauss-Lobatto-Legendre (GLL) points inside each box (Fig. 2). GLL points are $N + 1$ roots of the Legendre polynomial of degree N. These points are not uniformly distributed and they tend to cluster near the border of an element. Similar to FEM, SEM solves differential equation for fluid and heat transfer by constructing stiffness and mass matrix.

A brief description of the spectral numerical scheme and the results, which were used to validate the new spectral element simulations, are given in [9].

Table 1: Computational domain, grid density, time step and averaging times.

Numerical scheme	$\mathbf{Re}_\tau$	**Domain**	**Grid**	**Modes**	**Time step**	**Averaging time**
		$L_x \times L_y \times L_z$	$N_x \times N_y \times N_z$		Δt^+	t^+
Spectral	180	$4\pi \times 2 \times \frac{4\pi}{3}$	128x129x128 fluid 128x80x128 solid	n/a	0.027	5400
Spectral elements			30x30x30 elements in fluid 30x15x30 in each solid wall	6	0.027	8100

4 RESULTS

Simulations of the turbulent flow were started with an average dimensionless velocity in the channel of around 20 and with imposed perturbations of various wavelengths. The initial simulation with the imposed synthetic initial conditions evolved into a stationary turbulent flow in roughly 10^5 time steps. After that time the so-called statistical steady state was achieved where the velocities in the channel fluctuated around the mean - time independent values. After this initial time interval the code was running for another $3 \cdot 10^5$ time steps. During this simulation, velocity and temperature fields were saved every 1000 time steps for separate statistical analysis. Various velocity and temperature statistics shown on the figures below were obtained with averaging over x and z wall-parallel directions, over time and also with respect to the two mirror halves in the y direction.

4.1 Flow Field

Careful comparison of the turbulent flow fields obtained with the spectral element method is needed because the grid of the spectral elements shown in Fig. 2 did not use particularly refined grid in the near wall region like all the previous DNS studies [4,5,6,8,9]. In spectral schemes [4,5,9], where Chebyshev polynomials are used in wall-normal direction, the near-wall grid refinement appears "naturally" due to the nature of the basic functions. However, more versatile spectral element method allows also less refined near-wall resolution, which is tested in the present work.

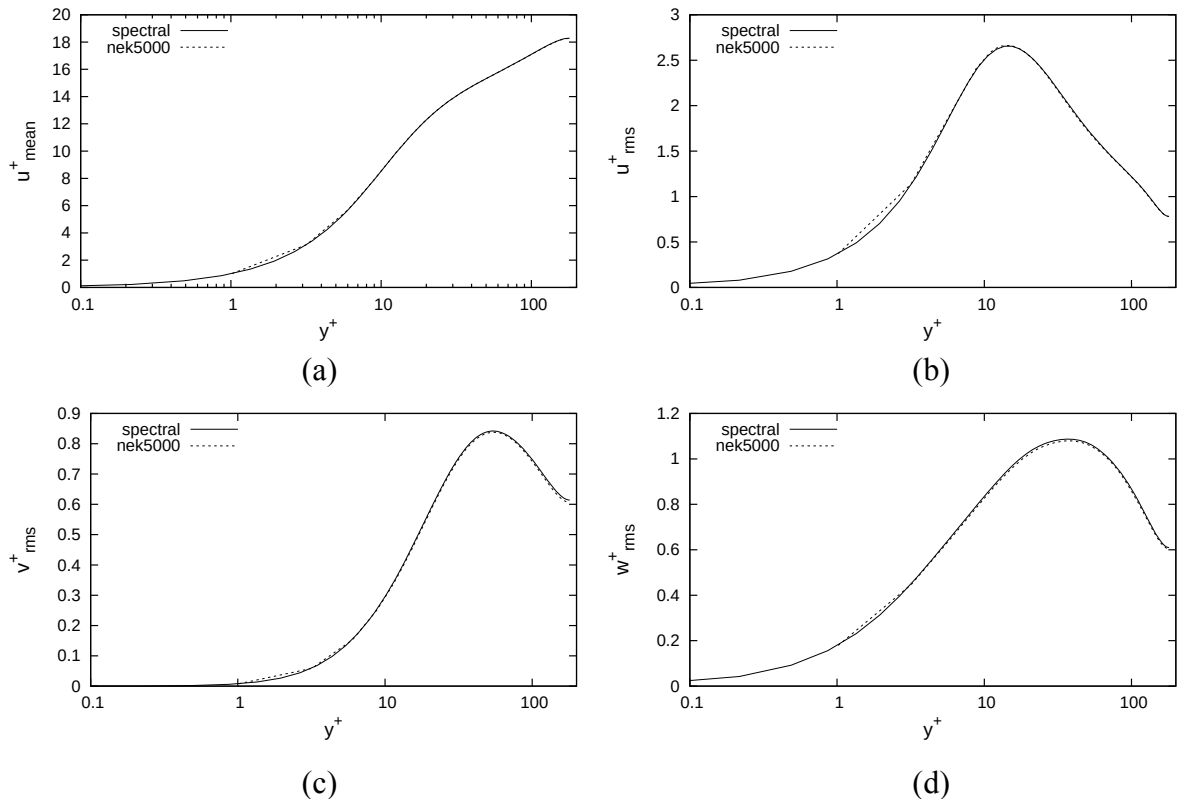

Figure 3: Comparison between spectral element scheme (Nek5000) and spectral scheme: (a) mean velocity, and (b, c, d) RMS fluctuations of components of velocities.

The key integral result of the simulations is the mean dimensionless velocity or the Reynolds number achieved in the channel at the specified constant pressure gradient. Our spectral method, which has been validated with other DNS results in [13] has obtained Reynolds number 5640 with accuracy of around 0.2%. The Reynolds number obtained with the Nek5000 code, simulated on the grid shown in Fig. 2 is the same: $\mathrm{Re}_\tau = 5643$.

Further comparison of the key velocity statistics is given in Fig. 3. Mean velocity profile, shown in the Fig. 3(a), points to a rather good agreement of spectral and spectral element results across the channel. One can see the piecewise linear structure of the spectral element solution on the logarithmic x-axis at $y^+ \lesssim 5$. Velocity RMS (root-mean-square) fluctuations shown in other three graphs of Fig. 3 also show agreement, which is expected for the DNS-quality of results. Typical relative difference between the peak values of the *u, v, w* RMS fluctuations are respectively 0.4%, -0.05%, -0.7%. Absolute values for calculated peaks are 2.6636, 0.8379, 0.1079 with Nek5000 code and 2.6536, 0.8418, 0.1087 with spectral code. These peak values were not obtained at exactly the same point due to mesh incompatibility and therefore matching could be further refined with the use of interpolation. However, this agreement supports our hypothesis that even the grid shown in Fig. 2, with coarse near-wall resolution, can produce DNS-quality results, since similar agreement is shown in [13] where various DNS results are compared. More detailed statistical analysis of the velocity field obtained on the Fig. 2 grid with spectral element code Nek5000 will be performed in the future and will confirm or reject our hypothesis that the implemented grid is sufficient for DNS.

4.2 Heat Transfer

Temperature field represents the key result of the present study. Since the temperature is a passive scalar in the present work, it does not affect the velocity field. The new approach for turbulent conjugate heat transfer simulations in complex geometries based on spectral elements is being validated in a simple channel flow geometry with the spectral code simulation mentioned in the Section 4.1. Mean temperature profiles in solid and liquid domains are shown in Fig. 4. Differences between the spectral scheme and spectral element scheme are too low to be seen at the given resolution. Mean dimensionless temperature shown in Fig. 4 is actually proportional to negative physical temperature, thus, the mean dimensionless temperature is negative in the solid and positive in the liquid. Due to the low Prandtl number of 0.01 and low Reynolds number, the log-law region in the temperature field does not appear; heat conductivity is much more important than turbulent transfer. Parabolic average temperature profile in the solid (Fig. 4(a)) can be obtained analytically.

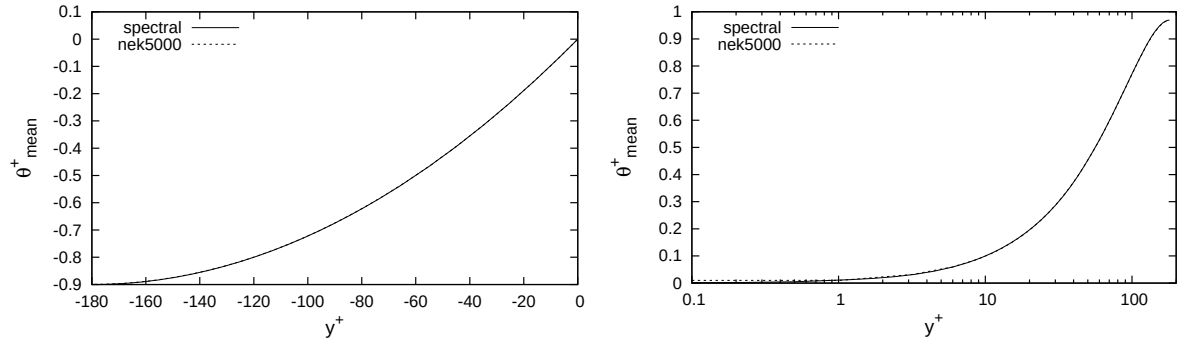

Figure 4: Mean temperature profiles in solid (a) and fluid (b).

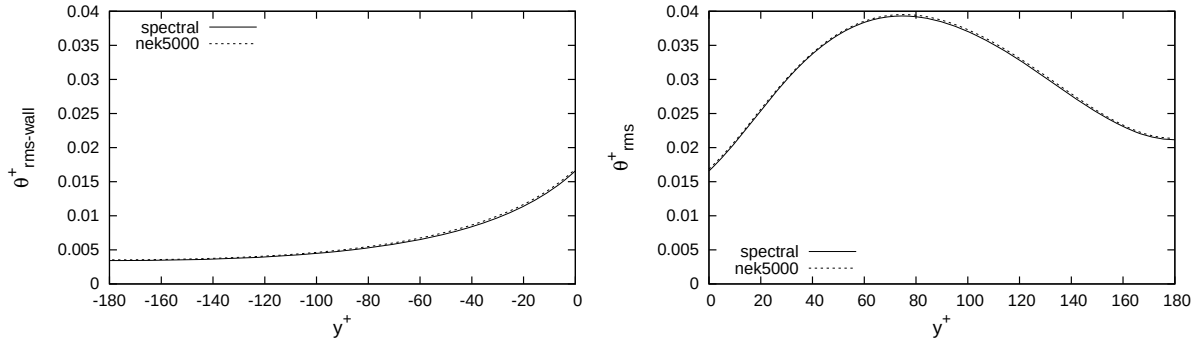

Figure 5: Temperature RMS fluctuations profiles in solid (a) and in fluid (b).

Fig. 5 shows RMS (root-mean-square) temperature fluctuations in the solid and in the fluid. Temperature fluctuations are created by the turbulence in the fluid, but they propagate also into the solid domain. These fluctuations are the key input quantities for prediction of the thermal fatigue. Good agreement between the results with two independent methods was obtained. Differences are barely visible at the given resolution. Nevertheless, these relative differences are slightly larger than differences in the corresponding velocity statistics shown in Fig. 3. Relative difference between the peak temperature RMS values in the fluid between both schemes is 2% (0.03952 with Nek5000 and 0.03884 with spectral). Relative differences in temperature RMS fluctuations at fluid-solid contact and at the isolated end of the solid are 2% and -3% respectively (0.1685, 0.03530 with Nek5000 and 0.1659, 0.03654 with spectral).

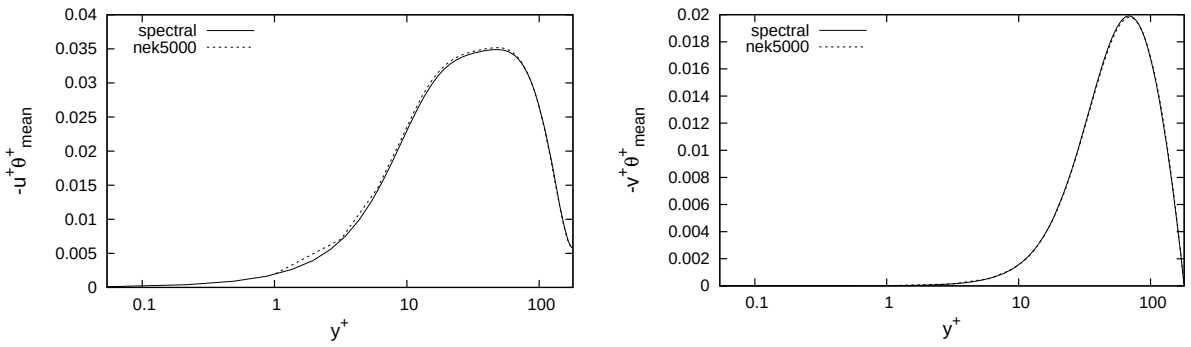

Figure 6: Streamwise (a) and wall-normal (b) turbulent heat fluxes.

Similar differences as in Fig. 5 can be seen in Fig. 6 which shows streamwise and wall-normal turbulent heat fluxes. Due to the low Prandtl number, wall normal turbulent heat fluxes are much lower than the corresponding Reynolds stress component that has a maximum close to 1.

5 CPU AND PARALLELIZATION

Comparing the computational time requirements of the spectral code and the newly applied spectral element code Nek5000 shows that the spectral scheme is much more efficient for the channel flow simulations.

With the spectral scheme it takes ~100 hours wall-clock time for $2 \cdot 10^5$ time steps on grid with $128 \times 129 \times 128$ modes (with convective terms calculated on 1.5 times expanded grid in each direction for dealiasing) with 15 scalar temperature fields of various wall properties. The simulation was running with in-house OpenMP parallelized code (applicable on shared memory systems only) on 2×6 cores with 2 threads (effectively 24 parallel threads). The key drawback of the OpenMP parallelization is that the code can only utilize the processors on a single node, i.e. typically several dozen parallel threads are maximum.

Spectral element scheme is significantly slower. It takes ~100 hours wall-clock time for $3 \cdot 10^5$ time steps on fluid grid $30 \times 60 \times 30$ elements - each element $7 \times 7 \times 7$ GLL points, which is roughly equal to $180 \times 180 \times 180$ points in each direction. The same number of spectral elements was used in solid domain for a single scalar field. MPI parallelization for distributed memory processors cannot be as effective as shared memory parallelization, but it allows utilization of much larger number of processors. For the present simulation the Nek5000 was running with 512 parallel threads on 64 processors (6 cores per processor, 2 threads per core). Optimum was achieved with reservation of 8 threads per processor.

Further tests will be needed to check whether the Nek5000 simulation, which is roughly 10 to 100 times slower per grid point and per time step than the spectral code on a single computing core, can be significantly accelerated. In any case, spectral element method allows massive parallel simulations and allows simulations in more complex geometries than spectral methods. Accuracy of the spectral element approach is comparable to the spectral scheme and is considered to be superior to the finite difference/volume approach.

6 CONCLUSIONS

Liquid metal turbulent heat transfer coupled with the unsteady conduction in the heated wall was analysed with the new numerical approach: spectral element method. Results were verified with pseudo spectral DNS in the same geometry of the infinite channel. Simulations were performed at friction Reynolds number $\mathrm{Re}_\tau = 180$ and Prandtl number $\mathrm{Pr} = 0.01$ and for walls with thickness equal to the half channel width and with equal material properties of liquid and solid. Good agreement between the methods was achieved.

In the future, we are planning to use the Nek5000 implementation of the spectral element method to simulate the flow across the backward facing step. The pseudo spectral method used for verification in this paper is unsuitable for such geometry. With this paper we verified the accuracy of the implementation. A possible improvement, which was not looked into, is the high computational time of Nek5000 code. However, as the aim was only to compare results, this optimisation will be performed with the new geometry.

ACKNOWLEDGMENTS

This project has received funding from the Euratom research and training programme 2014-2018 under grant agreement No 654935 and from the Ministry of Higher Education, Science and Technology, Republic of Slovenia, Research programme P-0026.

NOMENCLATURE

c_p = specific heat at constant pressure
d = wall thickness
G = α_f/α_w ratio of thermal diffusivities
h = channel half width
k = wave number
K = $\sqrt{\rho_f c_{pf} \lambda_f / \rho_w c_{pw} \lambda\_w}$ thermal activity ratio
L_x, L_z = streamwise and spanwise length of comput. domain
p = pressure
Pr = Prandtl number
q_w = wall-to-fluid heat flux
Re_τ = hu_τ/ν Friction Reynolds number
t = time
T_τ = $q_w/(u_\tau \rho_f c_{pf})$ friction temperature
$u, u_i,$ = velocity vector and components in i direction
u_τ = $\sqrt{\tau_w/\rho}$ friction velocity
u_B = bulk mean velocity
x = streamwise direction
y = wall-normal direction
z = spanwise direction
α = $\lambda/(\rho c_p)$thermal diffusivity
$\delta_{i,j}$ = 1 for $i = j$, 0 otherwise
θ = $(T_w - T)/T_\tau$ dimensionless temperature difference
λ = thermal conductivity
ν = kinematic viscosity
ρ = density
$\mathbf{1}_x$ = unit vector in x direction (1,0,0)

Subscripts and superscripts
$()_w$ = solid wall
$()_f$ = fluid
i,j = x and z direction wave number index
$()^+$ = normalized by u_τ, T_τ, ν
RMS = root-mean-square fluctuations averaged over x, z, t

REFERENCES

[1] Moin, P., Mahesh, K., 1999. Direct Numerical Simulation: A Tool in Turbulence Research. Annual Review of Fluid Mechanics, Vol. 30, pp. 539-578.

[2] Brillant, G., Husson, S., Bataille, F., Subgrid-scale diffusivity: wall behaviour and dynamic methods, J. Appl. Mech., Trans ASME, 73(3):360-367, 2006.

[3] Aulery, F., Toutant, A., Brillant, G., Monod, R., Bataille, F., Numerical simulations of sodium mixing in a T-junction, Appl. Therm. Eng., 37:38-43, 2012.

[4] Kim, J., Moin, P., 1989. Transport of Passive Scalars in a Turbulent Channel Flow. Turbulent Shear Flows VI, Springer-Verlag, Berlin, pp. 85.

[5] Kasagi, N., Tomita, Y., Kuroda, A., 1992. Direct Numerical Simulation of Passive Scalar Field in a Turbulent Channel Flow. Jornal of Heat Transfer -Transactions of ASME, Vol. 114, 598-606.

[6] Kawamura, H., Ohsaka, K, Abe, H., Yamamoto, K., 1998. DNS of Turbulent Heat Transfer in Channel Flow with low to medium-high Prandtl number fluid. International Journal of Heat and Fluid Flow, Vol. 19, 482-491.

[7] Polyakov, A.F., 1974. Wall Effect of Temperature Fluctuations in the Viscous Sublayer", Teplofizika Vysokih Temperatur. Vol. 12, pp.328-337.

[8] Tiselj, I., Bergant, R., Mavko, B., Bajsič, I., Hetsroni, G., 2001. DNS of Turbulent Heat Transfer in Channel Flow With Heat Conduction in the Solid Wall. Journal of Heat Transfer - ASME, 123, 849-857.

[9] Tiselj, I., Cizelj, L., 2012. DNS of turbulent channel flow with conjugate heat transfer at Prandtl number 0.01, Nuclear Engineering and Design 253 (2012) 153– 160.

[10] Fischer, P.F., Lottes, J.W., Kerkemeier, S.G., 2008. Nek5000 web page. (accessed 27. August 2015)

[11] Monod, R., Brillant, G., Toutant, A., Batailleb, F., 2012. Dimensionless equations for conjugate heat transfers. Submitted to Int. Com. Heat Mass Trans.

[12] Ampuero, J.P., 2009. www.gps.caltech.edu/~ampuero/docs/GE263_lecture_notes.pdf, California Institute of Technology, Lecture notes: GE 263 – Computational Geophysics: The spectral element method (accessed 27. August 2015)

[13] Komen, E., Shams, A., Camilo, L., Koren, B. 2014. Quasi-DNS capabilities of OpenFOAM for different mesh types, Computers & Fluids 96 (2014) 87–104.